

# On the Production of an Isotensor Dibaryon in the $pp \rightarrow pp\pi^+\pi^-$ Reaction

P. Adlarson,<sup>1</sup> W. Augustyniak,<sup>2</sup> W. Bardan,<sup>3</sup> M. Bashkanov,<sup>4</sup> F.S. Bergmann,<sup>5</sup> M. Berłowski,<sup>6</sup> A. Bondar,<sup>7,8</sup> M. Büscher,<sup>9,10</sup> H. Calén,<sup>1</sup> I. Ciepał,<sup>11</sup> H. Clement,<sup>12,13</sup> E. Czerwiński,<sup>3</sup> K. Demmich,<sup>5</sup> R. Engels,<sup>14</sup> A. Erven,<sup>15</sup> W. Erven,<sup>15</sup> W. Eyrich,<sup>16</sup> P. Fedorets,<sup>14,17</sup> K. Föhl,<sup>18</sup> K. Fransson,<sup>1</sup> F. Goldenbaum,<sup>14</sup> A. Goswami,<sup>14,19</sup> K. Grigoryev,<sup>14,20</sup> L. Heijckenskjöld,<sup>1,\*</sup> V. Hejny,<sup>14</sup> N. Hüskens,<sup>5</sup> L. Jarczyk,<sup>3</sup> T. Johansson,<sup>1</sup> B. Kamys,<sup>3</sup> G. Kemmerling,<sup>15,†</sup> A. Khoukaz,<sup>5</sup> O. Khreptak,<sup>3</sup> D.A. Kirillov,<sup>21</sup> S. Kistryn,<sup>3</sup> H. Kleines,<sup>15,†</sup> B. Kłos,<sup>22</sup> W. Krzemień,<sup>6</sup> P. Kulesa,<sup>11</sup> A. Kupść,<sup>1,6</sup> K. Lalwani,<sup>23</sup> D. Lersch,<sup>14,‡</sup> B. Lorentz,<sup>14</sup> A. Magiera,<sup>3</sup> R. Maier,<sup>14,24</sup> P. Marciniowski,<sup>1</sup> B. Mariański,<sup>2</sup> H.-P. Morsch,<sup>2</sup> P. Moskal,<sup>3</sup> H. Ohm,<sup>14</sup> W. Parol,<sup>11</sup> E. Perez del Rio,<sup>12,13,§</sup> N.M. Piskunov,<sup>21</sup> D. Prasuhn,<sup>14</sup> D. Pszczel,<sup>1,6</sup> K. Pysz,<sup>11</sup> J. Ritman,<sup>14,24,25</sup> A. Roy,<sup>19</sup> Z. Rudy,<sup>3</sup> O. Rundel,<sup>3</sup> S. Sawant,<sup>26</sup> S. Schadmand,<sup>14</sup> I. Schätti-Ozerianska,<sup>3</sup> T. Sefzick,<sup>14</sup> V. Serdyuk,<sup>14</sup> B. Shwartz,<sup>7,8</sup> T. Skorodko,<sup>12,13,27</sup> M. Skurzok,<sup>3</sup> J. Smyrski,<sup>3</sup> V. Sopov,<sup>17</sup> R. Stassen,<sup>14</sup> J. Stepaniak,<sup>6</sup> E. Stephan,<sup>22</sup> G. Sterzenbach,<sup>14</sup> H. Stockhorst,<sup>14</sup> H. Ströher,<sup>14,24</sup> A. Szczurek,<sup>11</sup> A. Trzciński,<sup>2</sup> M. Wolke,<sup>1</sup> A. Wrońska,<sup>3</sup> P. Wüstner,<sup>15</sup> A. Yamamoto,<sup>28</sup> J. Zabierowski,<sup>29</sup> M.J. Zieliński,<sup>3</sup> J. Złomańczuk,<sup>1</sup> J. Złomańczuk,<sup>1</sup> P. Żuprański,<sup>2</sup> and M. Żurek<sup>14</sup>

(WASA-at-COSY Collaboration)

- <sup>1</sup>Division of Nuclear Physics, Department of Physics and Astronomy, Uppsala University, Box 516, 75120 Uppsala, Sweden  
<sup>2</sup>Nuclear Physics Division, National Centre for Nuclear Research, ul. Hoza 69, 00-681, Warsaw, Poland  
<sup>3</sup>Institute of Physics, Jagiellonian University, prof. Stanisława Łojasiewicza 11, 30-348 Kraków, Poland  
<sup>4</sup>School of Physics and Astronomy, The University of Edinburgh, James Clerk Maxwell Building, Peter Guthrie Tait Road, Edinburgh EH9 3FD, Great Britain  
<sup>5</sup>Institut für Kernphysik, Westfälische Wilhelms-Universität Münster, Wilhelm-Klemm-Str. 9, 48149 Münster, Germany  
<sup>6</sup>High Energy Physics Division, National Centre for Nuclear Research, ul. Hoza 69, 00-681, Warsaw, Poland  
<sup>7</sup>Budker Institute of Nuclear Physics of SB RAS, 11 Acad. Lavrentieva Pr., Novosibirsk, 630090 Russia  
<sup>8</sup>Novosibirsk State University, 2 Pirogova Str., Novosibirsk, 630090 Russia  
<sup>9</sup>Peter Grünberg Institut, PGI-6 Elektronische Eigenschaften, Forschungszentrum Jülich, 52425 Jülich, Germany  
<sup>10</sup>Institut für Laser- und Plasmaphysik, Heinrich Heine Universität Düsseldorf, Universitätsstr. 1, 40225 Düsseldorf, Germany  
<sup>11</sup>The Henryk Niewodniczański Institute of Nuclear Physics, Polish Academy of Sciences, ul. Radzikowskiego 152, 31-342 Kraków, Poland  
<sup>12</sup>Physikalisches Institut, Eberhard Karls Universität Tübingen, Auf der Morgenstelle 14, 72076 Tübingen, Germany  
<sup>13</sup>Kepler Center for Astro and Particle Physics, Physikalisches Institut der Universität Tübingen, Auf der Morgenstelle 14, 72076 Tübingen, Germany  
<sup>14</sup>Institut für Kernphysik, Forschungszentrum Jülich, 52425 Jülich, Germany  
<sup>15</sup>Zentralinstitut für Engineering, Elektronik und Analytik, Forschungszentrum Jülich, 52425 Jülich, Germany  
<sup>16</sup>Physikalisches Institut, Friedrich-Alexander Universität Erlangen-Nürnberg, Erwin-Rommel-Str. 1, 91058 Erlangen, Germany  
<sup>17</sup>Institute for Theoretical and Experimental Physics named by A.I. Alikhanov of National Research Centre “Kurchatov Institute”, 25 Bolshaya Cheremushkinskaya Str., Moscow, 117218 Russia  
<sup>18</sup>II. Physikalisches Institut, Justus-Liebig-Universität Gießen, Heinrich-Buff-Ring 16, 35392 Giessen, Germany  
<sup>19</sup>Discipline of Physics, Indian Institute of Technology Indore, Khandwa Road, Indore, Madhya Pradesh 453 552, India  
<sup>20</sup>High Energy Physics Division, Petersburg Nuclear Physics Institute named by B.P. Konstantinov of National Research Centre “Kurchatov Institute”, 1 mkr. Orlova roshcha, Leningradskaya Oblast, Gatchina, 188300 Russia  
<sup>21</sup>Veksler and Baldin Laboratory of High Energy Physics, Joint Institute for Nuclear Physics, 6 Joliot-Curie, Dubna, 141980 Russia  
<sup>22</sup>August Chelkowski Institute of Physics, University of Silesia, ul. 75 Pułku Piechoty 1, 41-500 Chorzów, Poland  
<sup>23</sup>Department of Physics, Malaviya National Institute of Technology Jaipur, JLN Marg, Jaipur, Rajasthan 302 017, India  
<sup>24</sup>JARA-FAME, Jülich Aachen Research Alliance, Forschungszentrum Jülich, 52425 Jülich, and RWTH Aachen, 52056 Aachen, Germany  
<sup>25</sup>Institut für Experimentalphysik I, Ruhr-Universität Bochum, Universitätsstr. 150, 44780 Bochum, Germany  
<sup>26</sup>Department of Physics, Indian Institute of Technology Bombay, Powai, Mumbai, Maharashtra 400 076, India  
<sup>27</sup>Department of Physics, Tomsk State University, 36 Lenin Ave., Tomsk, 634050 Russia  
<sup>28</sup>High Energy Accelerator Research Organisation KEK, Tsukuba, Ibaraki 305-0801, Japan  
<sup>29</sup>Astrophysics Division, National Centre for Nuclear Research, Box 447, 90-950 Łódź, Poland

(Dated: April 19, 2018)

Exclusive measurements of the quasi-free  $pp \rightarrow pp\pi^+\pi^-$  reaction have been performed by means of  $pd$  collisions at  $T_p = 1.2$  GeV using the WASA detector setup at COSY. Total and differential cross sections have been obtained covering the energy region  $T_p = 1.08 - 1.36$  GeV ( $\sqrt{s} = 2.35 - 2.46$  GeV), which includes the regions of  $N^*(1440)$  and  $\Delta(1232)\Delta(1232)$  resonance excitations. Calculations describing these excitations by  $t$ -channel meson exchange are at variance with experimental differential cross sections and underpredict substantially the measured total cross section. An isotensor  $\Delta N$  dibaryon resonance with  $I(J^P) = 2(1^+)$  produced associatedly with a pion is

able to overcome these deficiencies. Such a dibaryon was predicted by Dyson and Xuong and more recently calculated by Gal and Garcilazo.

PACS numbers: 13.75.Cs, 14.20.Gk, 14.20.Pt

Keywords: Two-Pion Production,  $\Delta\Delta$  Excitation, Roper Resonance, Dibaryon Resonance

## I. INTRODUCTION

Early measurements of two-pion production initiated by nucleon-nucleon ( $NN$ ) collisions were conducted with bubble-chambers, where due to low statistics primarily only results for total cross sections were obtained [1–7].

In recent years the two-pion production has been measured from threshold up to incident energies of  $T_p = 1.4$  GeV with high-accuracy by exclusive and kinematically complete experiments conducted at CELSIUS [8–16], COSY [17–24], GSI [25] and JINR [26]. Whereas initially proton-proton ( $pp$ ) induced two-pion production was the primary aim of these measurements [8–15, 17–19], the interest moved later to proton-neutron ( $pn$ ) induced reaction channels – after the first clear-cut evidence for a dibaryon resonance with  $I(J^P) = 0(3^+)$  had been observed in the  $pn \rightarrow d\pi^0\pi^0$  reaction [16, 20, 21]. Subsequent measurements of the  $pn \rightarrow d\pi^+\pi^-$  [22],  $pn \rightarrow pp\pi^0\pi^-$  [23],  $np \rightarrow np\pi^0\pi^0$  [24] and  $pn \rightarrow pn\pi^+\pi^-$  [25, 27] reactions revealed that all two-pion production channels, which contain isoscalar contributions, exhibit a signal of this resonance — now called  $d^*(2380)$  after observation of its pole in  $pn$  scattering [28–30].

Aside from the dibaryon resonance phenomenon the standard theoretical description of the two-pion production process at the energies of interest here is dominated by  $t$ -channel meson exchange leading to excitation and decay of the Roper resonance  $N^*(1440)$  and of the  $\Delta(1232)\Delta(1232)$  system [31, 32]. At lower incident energies the Roper excitation dominates. At incident energies beyond 1 GeV the  $\Delta\Delta$  process takes over. Such calculations give quite a reasonable description of the data — with the big exception of the  $pp \rightarrow pp\pi^0\pi^0$  cross section above 1 GeV. After readjusting the decay branching of the Roper resonance used in these calculations to that obtained in recent analyses of data on pion- and photon-induced two-pion production [33, 34], a quantitative description of total and differential cross section data was achieved for both the  $pp \rightarrow pp\pi^0\pi^0$  and the  $pp \rightarrow pp\pi^+\pi^-$  reactions at incident energies below 0.9 GeV [8–11, 19], where the Roper excitation dominates.

For a quantitative description of the  $pp \rightarrow pp\pi^0\pi^0$  data above 1 GeV, however, the calculation of the  $\Delta\Delta$  process as used originally in Ref. [31] had to be modified [14], in particular the  $\rho$  exchange contribution had to be strongly reduced. Also, the strength of the Roper excitation had to be reduced in accord with isospin decomposition [12], and in order to describe the  $pp \rightarrow nn\pi^+\pi^+$  reaction quantitatively, a contribution from a higher-lying broad  $\Delta$  resonance, *e.g.*, the  $\Delta(1600)$ , had to be assumed [15]. These calculations, called now "modified Valencia" calculations give a good description of all data in  $pp$ -induced and also of  $pn$ -induced channels – if in the latter the  $d^*(2380)$  resonance is taken into account – with one striking exception: the  $pp \rightarrow pp\pi^+\pi^-$  total cross section data beyond 0.9 GeV are strongly underpredicted (see dashed line in Fig. 4). This problem was already noted in the isospin decomposition of  $pp$ -induced two-pion production [12]. However, since all the  $pp \rightarrow pp\pi^+\pi^-$  data beyond 0.8 GeV stem from early low-statistics bubble-chamber measurements, it appears appropriate to reinvestigate this region by exclusive and kinematically complete measurements.

There is yet another point of interest in this reaction at energies above 0.8 GeV. Dyson and Xuong [35] were the first, who properly predicted the dibaryon resonances  $d^*(2380)$  (called  $D_{IJ} = D_{03}$  by Dyson and Xuong) and  $D_{12}$ , the latter denoting a slightly bound  $\Delta N$  threshold state with  $I(J^P) = 1(2^+)$ . For a recent discussion about that state see *e.g.* Ref. [36] and references therein. According to Dyson and Xuong, as well as to recent Faddeev calculations performed by Gal and Garcilazo [37], there should be yet another  $\Delta N$  threshold state with  $I(J^P) = 2(1^+)$ , called  $D_{21}$  in Ref. [35]. Because of its large isospin of  $I = 2$ , this state cannot be excited directly by incident  $NN$  collisions, but only associatedly – favorably by production of an additional pion, which carries away one unit of isospin. By isospin selection the decay of an isotensor  $\Delta N$  state will dominantly proceed into the purely isotensor  $pp\pi^+$  channel. Hence the  $pp \rightarrow pp\pi^+\pi^-$  reaction is the ideal place to look for the process  $pp \rightarrow D_{21}^{++}\pi^- \rightarrow pp\pi^+\pi^-$  – as already suggested in Ref. [35]. The main results of this investigation have been communicated recently in a Letter [38].

## II. EXPERIMENT

The reaction  $pp \rightarrow pp\pi^+\pi^-$  was measured by use of the quasifree process in  $pd$  collisions. The experiment was carried out at COSY (Forschungszentrum Jülich) with the WASA detector setup by using a proton beam with an energy of  $T_p = 1.2$  GeV impinging on a deuterium

\*present address: Institut für Kernphysik, Johannes Gutenberg Universität Mainz, Johann-Joachim-Becher Weg 45, 55128 Mainz, Germany

†present address: Jülich Centre for Neutron Science JCNS, Forschungszentrum Jülich, 52425 Jülich, Germany

‡present address: Department of Physics, Florida State University, 77 Chieftan Way, Tallahassee, FL 32306-4350, USA

§present address: INFN, Laboratori Nazionali di Frascati, Via E. Fermi, 40, 00044 Frascati (Roma), Italy

pellet target [39, 40]. By exploiting the Fermi motion in the target deuteron by the quasi-free scattering process  $pd \rightarrow pp\pi^+\pi^- + n_{spectator}$ , we cover the energy region  $T_p = 1.08 - 1.36$  GeV ( $\sqrt{s} = 2.35 - 2.46$  GeV) of the  $pp \rightarrow pp\pi^+\pi^-$  reaction.

The hardware trigger utilized in this analysis required two charged hits in the forward detector as well as two recorded hits in the central detector.

The reaction  $pd \rightarrow pp\pi^+\pi^- + n$  was selected in the offline analysis by requiring two proton tracks in the forward detector as well as a  $\pi^+$  and  $\pi^-$  track in the central detector.

That way, the unmeasured neutron four-momentum could be reconstructed by a kinematic fit with one over-constraint. The achieved resolution in  $\sqrt{s}$  was about 20 MeV.

The charged particles registered in the segmented forward detector of WASA have been identified by use of the  $\Delta E - E$  energy loss method. For its application in the data analysis, all combinations of signals stemming from the five layers of the forward range hodoscope have been used. The charged particles in the central detector have been identified by their curved track in the magnetic field as well as by their energy loss in the surrounding plastic scintillator barrel and electromagnetic calorimeter.

The momentum distribution of the reconstructed neutron is shown in Fig. 1. The dashed curve gives the expected momentum distribution for a spectator neutron according to the deuteron wavefunction based on the CD Bonn potential [41]. Compared to previous measurements on  $d\pi^0\pi^0$  [20],  $d\pi^+\pi^-$  [22],  $np\pi^0\pi^0$  [24] and  $pp\pi^0\pi^-$  [23] channels we find here a somewhat enhanced background from non-spectator contributions. In order to keep these background contributions smaller than 2%, we would need to restrict the spectator momentum range to  $p < 0.10$  GeV/c. But such a cut would severely reduce the covered energy range to  $1.15$  GeV  $< T_p < 1.3$  GeV ( $2.38$  GeV  $< \sqrt{s} < 2.44$  GeV). To reliably evaluate the data up to  $p = 0.15$  GeV/c for the quasifree reaction – as done in our previous analyses – we decided to perform a proper background correction by analyzing additionally the non-spectator reaction process by evaluating the data in the non-overlap region  $p_n > 0.25$  GeV/c.

The requirement that the two protons have to be in the angular range covered by the forward detector and that  $\pi^+$  and  $\pi^-$  have to be in the angular range of the central detector reduces the overall acceptance to about 30% in case of the quasifree process and to about 5% in case of the non-quasifree reaction. The total reconstruction efficiency including all cuts and conditions has been 1.1% for the quasifree process and about 0.2% for the non-quasifree process. In total a sample of about 26000 events has been selected meeting all cuts and conditions for the quasifree process  $pd \rightarrow pp\pi^+\pi^- + n_{spectator}$ . For  $p > 0.25$  GeV/c in the region of the non-quasifree process this number is about 20000.

Efficiency and acceptance corrections of the data have been performed by MC simulations of reaction process

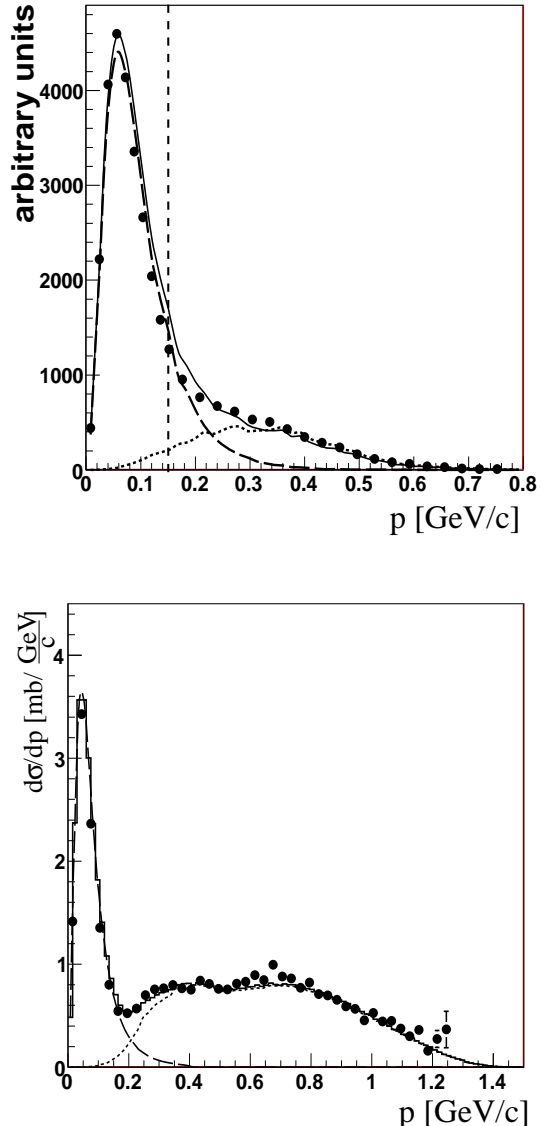


FIG. 1: (Color online) Distribution of the neutron momenta in the  $pd \rightarrow npp\pi^+\pi^-$  reaction before (top) and after acceptance and efficiency correction (bottom). Data are given by solid dots. The dashed line shows the expected distribution for the quasifree process  $pd \rightarrow pp\pi^+\pi^- + n_{spectator}$  based on the CD Bonn potential [41] deuteron wavefunction. The vertical line indicates the region  $p < 0.15$  GeV/c used for the evaluation of the quasifree process. The dotted line gives the modeling of the non-quasifree reaction process. The solid line is the incoherent sum of both processes.

and detector setup. For the MC simulations pure phase-space and model descriptions have been used, which will be discussed below. Since WASA does not cover the full reaction phase space, albeit a large fraction of it, these corrections are not fully model independent. The hatched grey histograms in Figs. 2 - 3 and 5 - 9 give an estimate for these systematic uncertainties. As a measure

of these we have taken the difference between model corrected results and those obtained by assuming pure phase space for the acceptance corrections in case of the non-spectator background reaction. In case of the quasifree  $pp \rightarrow pp\pi^+\pi^- + n_{spectator}$  reaction we use the difference between the results obtained with the final model and those using the "modified Valencia" model for the acceptance correction. Compared to the uncertainties in these corrections, systematic errors associated with modeling the reconstruction of particles are negligible.

The absolute normalization of the data has been obtained by comparison of the quasi-free single pion production process  $pd \rightarrow pp\pi^0 + n_{spectator}$  to previous bubble-chamber results for the  $pp \rightarrow pp\pi^0$  reaction [3, 5]. That way, the uncertainty in the absolute normalization of our data is essentially that of the previous  $pp \rightarrow pp\pi^0$  data, *i.e.* in the order of 5 - 15%.

### III. THE NON-SPECTATOR BACKGROUND PROCESS $pd \rightarrow ppn\pi^+\pi^-$

For an axially symmetric five-body final state there are eleven independent differential observables. For the non-spectator background reaction  $pd \rightarrow ppn\pi^+\pi^-$  we show in Figs. 2 and 3 twelve differential observables: the invariant mass distributions  $M_{pp}$ ,  $M_{pn}$ ,  $M_{p\pi^+}$ ,  $M_{n\pi^-}$ ,  $M_{p\pi^-}$ ,  $M_{n\pi^+}$ ,  $M_{\pi^+\pi^-}$  and  $M_{pn\pi^+\pi^-}$  as well as the angular distributions for protons ( $\Theta_p^{c.m.}$ ), neutrons ( $\Theta_n^{c.m.}$ ), positive pions ( $\Theta_{\pi^+}^{c.m.}$ ) and negative pions ( $\Theta_{\pi^-}^{c.m.}$ ).

The obtained differential distributions deviate partly substantially from pure phase-space distributions. This is the case in particular for the distributions of the invariant masses  $M_{p\pi^+}$  and  $M_{n\pi^-}$  exhibiting the excitations of  $\Delta^{++}$  and  $\Delta^-$ , as well as of the angles  $\Theta_p^{c.m.}$ ,  $\Theta_n^{c.m.}$ ,  $\Theta_{\pi^-}^{c.m.}$  and  $\Theta_{\pi^+}^{c.m.}$ . However, all differential distributions fit well to a modeling of the process  $pd \rightarrow N\Delta\Delta \rightarrow ppn\pi^+\pi^-$ . Since it proceeds dominantly via the  $\Delta^{++}\Delta^-$  configuration due to isospin selection, the  $M_{p\pi^+}$  and  $M_{n\pi^-}$  spectra peak at the  $\Delta$  mass, as we observe in Fig. 2. The pion angular distributions are as expected from the  $p$ -wave decay of the intermediate  $\Delta$  resonances. Proton and neutron angular distributions are strongly curved as expected from a peripheral collision. In comparison to the neutron angular distribution, the proton angular distribution appears to be less anisotropic, since only one of the two protons is dominantly active.

The success of such a background modeling is of no great surprise, since the  $pn\pi^+\pi^-$  channel has the by far largest two-pion production cross section. Also we know from the  $pd \rightarrow {}^3\text{He}\pi\pi$  reaction, where the  $ppn$  system has fused to  ${}^3\text{He}$ , that for  $T_p > 1$  GeV the  $t$ -channel  $\Delta\Delta$  process is by far dominating [42]. As in the latter case we observe also here the  $\Delta$  signals in the invariant mass spectra to be somewhat broadened, which may be traced back to the Fermi motion of the participating nucleons and may be accounted for most easily by increasing the  $\Delta$  width from 120 to 140 MeV by a fit to the data.

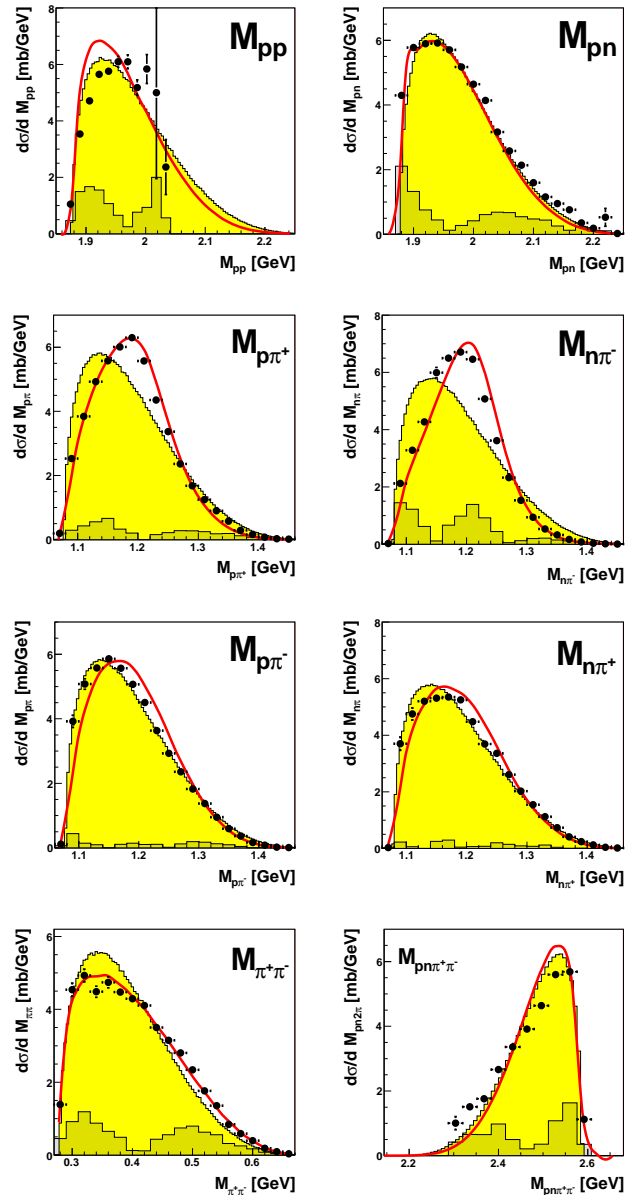


FIG. 2: (Color online) Differential distributions of the non-spectator background reaction  $pd \rightarrow ppn\pi^+\pi^-$  for the invariant mass distributions  $M_{pp}$ ,  $M_{pn}$ ,  $M_{p\pi^+}$ ,  $M_{n\pi^-}$ ,  $M_{p\pi^-}$ ,  $M_{n\pi^+}$ ,  $M_{\pi^+\pi^-}$  and  $M_{pn\pi^+\pi^-}$  for  $p_n > 0.2$  GeV/c. The shaded areas represent pure phase-space distributions. The hatched areas indicate systematic uncertainties due to the restricted phase-space coverage in the measurement. The solid curves give a modeling of the process  $pd \rightarrow ppn\pi^+\pi^-$ .

Having achieved a quantitative description of the non-quasifree background process for  $p_n > 0.25$  GeV/c, we may extrapolate its contribution reliably also for  $p_n < 0.15$  GeV/c and subtract it from the measured neutron momentum distribution (Fig. 1), in order to obtain the pure quasi-free part, which is of main interest here.

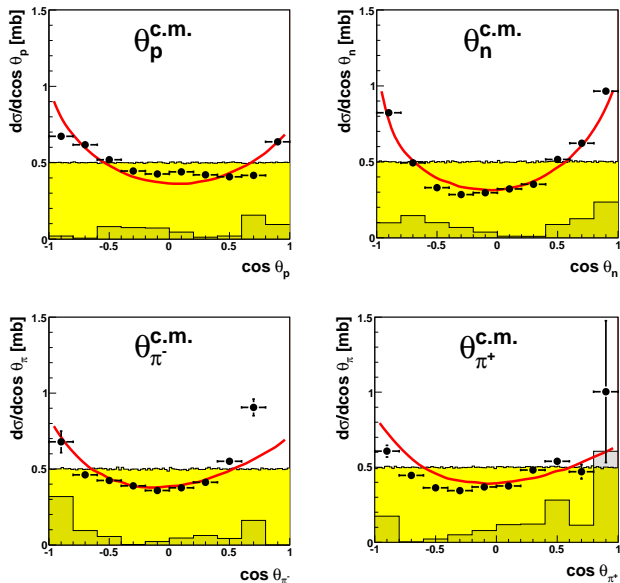


FIG. 3: (Color online) Same as Fig 2, but for the angular distributions of protons ( $\Theta_p^{c.m.}$ ), neutrons ( $\Theta_n^{c.m.}$ ), positive pions ( $\Theta_{\pi^+}^{c.m.}$ ) and negative pions ( $\Theta_{\pi^-}^{c.m.}$ ).

#### IV. THE QUASIFREE REACTION

$$pp \rightarrow pp\pi^+\pi^- + n_{spectator}$$

##### A. Total cross section

In order to determine the energy dependence of total and differential cross sections for the quasi-free process of interest, we have divided our background subtracted data into bins of 50 MeV width in the incident energy  $T_p$ . The resulting total cross sections are shown in Fig. 4 (solid circles) together with results from earlier measurements (other symbols) [2–4, 8–10, 19]. Our data for the total cross section are in reasonable agreement with the earlier measurements in the considered energy region.

In order to compare with theoretical expectations we first plot in Fig. 4 the results of the original Valencia calculations [31] by the dotted line. At first glance the agreement with the data appears remarkable. However, as mentioned in the introduction, these calculations are far off for the  $pp\pi^0\pi^0$  channel. The so-called "modified Valencia" calculations, which account reasonably well for the latter channel, are shown in Fig. 4 by the dashed line. These calculations do very well at low energies, but yield a much too low cross section at higher energies. The reason is that by isospin relations the energy dependences of  $pp\pi^0\pi^0$  and  $pp\pi^+\pi^-$  channels have to be qualitatively similar, if only  $t$ -channel Roper and  $\Delta\Delta$  processes contribute, since then the matrix element  $M_{I_{pp}^f I_{\pi^+\pi^-}^i} = M_{111}$  ( $\rho$ -channel in the  $\pi^+\pi^-$  subsystem) vanishes [57] [12, 43]. So, if the kink around  $T_p \approx 1.1$  GeV in the  $pp\pi^0\pi^0$  data [14] got to be reproduced by such model calculations, then also the  $pp\pi^+\pi^-$  channel

has to behave similarly, if only these two processes are at work.

In the total cross section the  $t$ -channel Roper and  $\Delta\Delta$  excitations interfere only weakly (see, *e.g.*, Fig. 3 in Ref. [31], where the cross sections of the individual processes are seen to just add up in good approximation). Hence we may neglect their interference terms in good approximation and obtain thus from isospin decomposition, eqs. (1) - (5) in Ref. [12] for the total cross sections of  $pp\pi^0\pi^0$  and  $pp\pi^+\pi^-$  channels:

$$\begin{aligned} \sigma_{pp\pi^0\pi^0} &\approx \sigma^{N^*} + \sigma^{\Delta\Delta} \\ \sigma_{pp\pi^+\pi^-} &\approx 2\sigma^{N^*} + \frac{9}{8}\sigma^{\Delta\Delta} + \frac{1}{8}|M_{111}|^2 \end{aligned} \quad (1)$$

where  $\sigma^{N^*}$  and  $\sigma^{\Delta\Delta}$  denote the cross sections of  $t$ -channel Roper and  $\Delta\Delta$  processes, respectively. Since the relative weight of the  $\Delta\Delta$  process is less than that of the Roper process in  $\sigma_{pp\pi^+\pi^-}$ , the kink near  $T_p \approx 1.1$  GeV is smaller than in  $\sigma_{pp\pi^0\pi^0}$ , but still present, because the  $\Delta\Delta$  process provides a much bigger cross section than the Roper process does.

We note in passing that in the article about isospin decomposition [12] the missing strength in the  $pp\pi^+\pi^-$  channel appeared still less dramatic, since at that time full interference between the isospin matrix elements for Roper and  $\Delta\Delta$  excitations was assumed. But as later model calculations showed, this interference is very small, since both excitations act on quite different phase-space volumes. For that reason interferences between the various resonance excitations have been omitted at all in the model calculations of Ref. [32].

The  $\Delta(1600)$  excitation also contributes to  $M_{111}$  albeit much too little in order to heal the deficit in the cross section. The "modified Valencia" calculations (dashed line in Fig. 4) do include this contribution.

In this context we also have to ask, whether possibly other higher-lying  $N^*$  and  $\Delta$  resonances provide substantial contributions in the energy region of interest here. This has been comprehensively investigated in Ref. [32] with the result that all of these (including also  $N^*(1520)$ ) give only negligible contributions to the two-pion production cross sections.

##### B. Differential cross sections

When binned into  $T_p$  bins of 50 MeV width, the differential distributions do not exhibit any particularly strong energy dependence in their shapes – which is of no surprise, since the energy region covered in this measurement is dominated by  $\Delta\Delta$  and Roper excitations with very smooth energy dependencies due to their large decay widths. Hence we discuss the differential distributions at first unbinned, *i.e.* averaged over the full covered energy range.



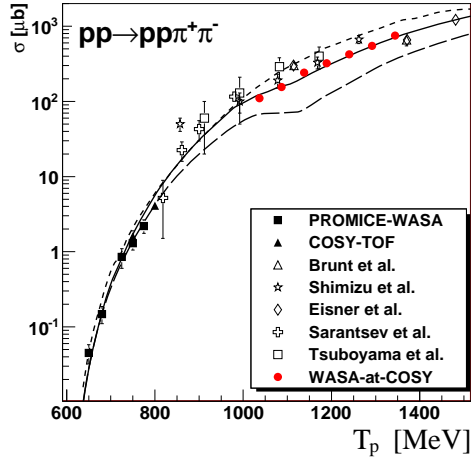


FIG. 4: (Color online) Total cross section in dependence of the incident proton energy  $T_p$  for the reaction  $pp \rightarrow pp\pi^+\pi^-$ . The solid dots show results from this work. Other symbols denote results from previous measurements [2–4, 8–10, 19]. The dotted line gives the original Valencia calculation [31], the dashed one the so-called "modified Valencia" calculation [14]. The solid line is obtained, if to the latter an associatedly produced  $D_{21}$  resonance is added according to the process  $pp \rightarrow D_{21}\pi^- \rightarrow pp\pi^+\pi^-$  with the strength of this process being fitted to the total cross section data.

For an axially symmetric four-body final state there are seven independent differential observables. For a better discussion of the physics issue we show in this paper nine differential distributions, those for the center-of-mass (c.m.) angles for protons and pions denoted by  $\Theta_p^{c.m.}$ ,  $\Theta_{\pi^+}^{c.m.}$  and  $\Theta_{\pi^-}^{c.m.}$ , respectively, as well as those for the invariant masses  $M_{pp}$ ,  $M_{\pi^+\pi^-}$ ,  $M_{p\pi^+}$ ,  $M_{pp\pi^+}$ ,  $M_{p\pi^-}$  and  $M_{pp\pi^-}$ . These distributions are shown in Figs. 5 and 6.

There are no data to compare with from previous experiments in the energy range considered here. All measured differential distributions differ markedly in shape from pure phase-space distributions (shaded areas in Figs. 5 - 6). With the exception of  $\Theta_{\pi^+}^{c.m.}$ ,  $M_{p\pi^-}$  and  $M_{pp\pi^-}$  spectra, the differential distributions are reasonably well reproduced by the "modified Valencia model" calculations (dashed curves). For the original Valencia calculation (dotted lines), which contains substantial contributions from the Roper excitation still in this energy region, large discrepancies get apparent in addition for the  $M_{\pi^+\pi^-}$  distribution. For better comparison all calculations are adjusted in area to the data in Figs. 5 - 9.

The proton angular distribution is forward-backward peaked as expected for a peripheral reaction process. The  $\pi^-$  angular distribution is flat, in tendency slightly convex curved – as predicted by the theoretical calculations – and as also observed in the other  $NN\pi\pi$  channels at these energies. But surprisingly, the  $\pi^+$  angular distribution exhibits a strikingly concave shape. Such a strange

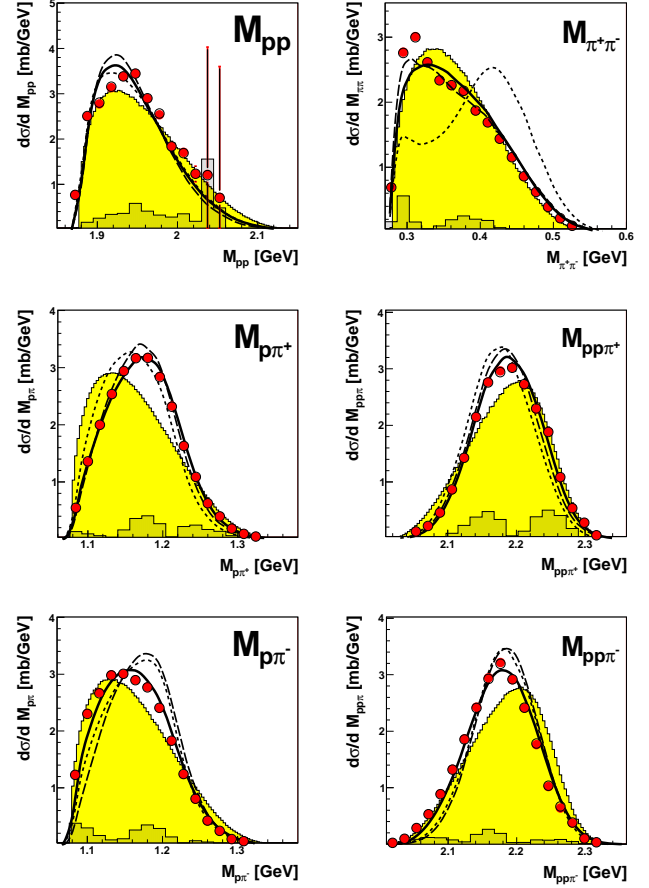


FIG. 5: (Color online) Differential distributions of the  $pp \rightarrow pp\pi^+\pi^-$  reaction in the region  $T_p = 1.08 - 1.36$  GeV for the invariant-masses  $M_{pp}$  (top left),  $M_{\pi^+\pi^-}$  (top right),  $M_{p\pi^+}$  (middle left),  $M_{pp\pi^+}$  (middle right),  $M_{p\pi^-}$  (bottom left),  $M_{pp\pi^-}$  (bottom right). Filled (open) circles denote the results from this work after (before) background subtraction. In most cases these symbols lie on top of each other. The hatched histograms indicate systematic uncertainties due to the restricted phase-space coverage of the data. The shaded areas represent pure phase-space distributions, dotted (dashed) lines represent original (modified) Valencia calculations [31] ([14]). The solid lines include the process  $pp \rightarrow D_{21}\pi^- \rightarrow pp\pi^+\pi^-$ . All calculations are normalized in area to the data.

behavior, which is in sharp contrast to the theoretical expectation, has been observed so far in none of the two-pion production channels.

Also the  $M_{p\pi^-}$  spectrum is markedly different from the  $M_{p\pi^+}$  spectrum. The same is true for the  $M_{pp\pi^-}$  spectrum with respect to the  $M_{pp\pi^+}$  distribution. In case of the  $t$ -channel  $\Delta\Delta$  process, which is thought to be the dominating one at the energies of interest here,  $\Delta^{++}$  and  $\Delta^0$  get excited simultaneously and with equal strengths. Hence, the  $M_{p\pi^+}$  ( $M_{pp\pi^+}$ ) spectrum should be equal to the  $M_{p\pi^-}$  ( $M_{pp\pi^-}$ ) one and also the  $\pi^+$  angular distribution should be the same as the  $\pi^-$  angular distribution.

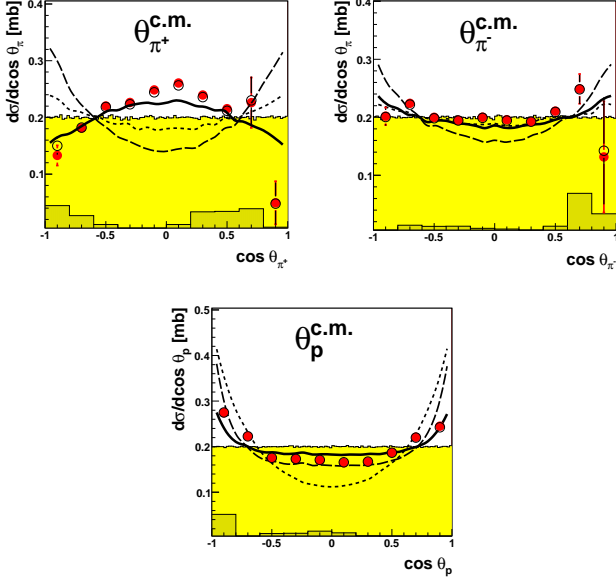


FIG. 6: (Color online) The same as Fig. 5, but for the c.m. angles of positive and negative pions  $\Theta_{\pi^+}^{c.m.}$  and  $\Theta_{\pi^-}^{c.m.}$ , respectively, as well as protons  $\Theta_p^{c.m.}$ .

So the failure of the "modified Valencia" calculation to describe properly the total cross section and the differential distributions underlines the suspicion that the  $t$ -channel  $\Delta\Delta$  process is not the leading process here.

Since the total cross section is grossly underpredicted above  $T_p \approx 1.0$  GeV, it appears that an important piece of reaction dynamics is missing, which selectively affects the  $pp\pi^+\pi^-$  channel. Furthermore, the discrepancy between data and "modified Valencia" description opens up scissor-like around  $T_p \approx 0.9$  GeV, which suggests the opening of a new channel, where a  $\Delta N$  system is produced associatedly with another pion. Such a state with the desired properties could be the isotensor  $D_{21}$  state with  $I(J^P) = 2(1^+)$  predicted already by Dyson and Xuong [35] with a mass close to that of its isospin partner  $D_{12}$  with  $I(J^P) = 1(2^+)$ . Whereas  $D_{12}$  can be reached directly by the initial  $pp$  channel,  $D_{21}$  cannot be reached that way because of its isospin  $I = 2$ . However, it can be produced in initial  $pp$  collisions associatedly with an additional pion.

### C. $D_{12}$ resonance

In several partial-wave analyses of  $pp$  and  $\pi d$  scattering as well as of the  $pp \rightarrow d\pi^+$  reaction the  $D_{12}$  resonance has been identified at a mass of 2144 - 2148 MeV [44, 45], *i.e.* with a binding energy of a few MeV relative to the nominal  $\Delta N$  threshold – and with a width compatible to that of the  $\Delta$  resonance. For a recent discussion about the nature of this  $D_{12}$  state see, *e.g.*, Ref. [36] and ref-

erences therein. Also recent Faddeev calculations for the  $NN\pi$  system find both  $D_{12}$  and  $D_{21}$  dibaryon resonances with masses slightly below the  $\Delta N$  threshold and with widths close to that of the  $\Delta$  resonance [37]. The decay of the  $D_{12}$  resonance proceeds dominantly into  $d\pi$  and  $np\pi$  channels, since there the  $np$  pair can reside in the  ${}^3S_1$  partial wave, which readily couples with the  $p$ -wave pion (from  $\Delta$  decay) to  $J^P = 2^+$ . In contrast, its decay into  $pp\pi$  is heavily suppressed, since the  $pp$  pair can couple only to  ${}^1S_0$  in relative  $s$ -wave and hence needs at least relative  $d$ -waves for building a  $J^P = 2^+$  state in the  $pp\pi$  system. Since it does not show up in the  $pp\pi$  system, it also will not appear in the  $pp \rightarrow pp\pi^+\pi^-$  reaction.

### D. $D_{21}$ resonance

The hypothetical isotensor state  $D_{21}$ , on the other hand, strongly favors the purely isotensor channel  $pp\pi^+$  in its decay. In addition,  $J^P = 1^+$  can be easily reached by adding a  $p$ -wave pion (from  $\Delta$  decay) to a  $pp$  pair in the  ${}^1S_0$  partial wave. Hence – as already suggested by Dyson and Xuong [35] – the favored production process should be in the  $pp \rightarrow pp\pi^+\pi^-$  reaction.

If we use the formalism outlined in Ref. [46], then the resonance process  $pp \rightarrow D_{21}\pi \rightarrow \Delta p\pi \rightarrow pp\pi\pi$  can be described by the transition amplitude

$$M_R(m_{p_1}, m_{p_2}, m_{p_3}, m_{p_4}, \hat{k}_1, \hat{k}_2) = M_R^0 \Theta_R(m_{p_1}, m_{p_2}, m_{p_3}, m_{p_4}, \hat{k}_1, \hat{k}_2), \quad (2)$$

where the function  $\Theta$  contains the substate and angular dependent part, and

$$M_R^0 = D_{D_{21}} * D_{\Delta} \quad (3)$$

with  $D_{D_{21}}$  and  $D_{\Delta}$  denoting the corresponding resonance propagators. Here  $p_1, p_2$  and  $p_3, p_4$  denote the ingoing and outgoing protons, respectively.  $k_1$  is the momentum of the associatedly produced pion and  $k_2$  that of the pion resulting from the decay  $D_{21} \rightarrow \Delta p \rightarrow pp\pi$

If the coordinate system is chosen to be the standard one with the  $z$ -axis pointing in beam direction (implying  $m_L = 0$  and  $(\Theta_i, \Phi_i) = (0, 0)$ ), then the function  $\Theta_R(m_p, m_n, m_{p_3}, m_{p_4}, \hat{k}_1, \hat{k}_2)$  defined in eq. (2) is built up by the corresponding vector coupling coefficients and spherical harmonics representing the angular dependence due to the orbital angular momenta involved in the reaction:

$$\Theta_R(m_{p_1}, m_{p_2}, m_{p_3}, m_{p_4}, \hat{k}_1, \hat{k}_2) = \sum \left( \frac{1}{2} \frac{1}{2} m_{p_1} m_{p_2} |S m_s\rangle (S L m_s 0 | J M) \right. \\ \left. (J M | J_{D_{21}} l m_{D_{21}} m_1) (J_{D_{21}} m_{D_{21}} | \frac{3}{2} \frac{1}{2} m_{\Delta} m_{p_3}) \right. \\ \left. (\frac{3}{2} m_{\Delta} | \frac{1}{2} 1 m_{p_4} m_2) Y_{L0}(0, 0) Y_{l m_1}(\hat{k}_1) Y_{1 m_2}(\hat{k}_2) \right). \quad (4)$$

The  $D_{21}$  resonance can be formed together with an associatedly produced pion either in relative  $s$  or  $p$  wave.

In the first instance the initial  $pp$  partial wave is  ${}^3P_1$ , in the latter one it is  ${}^1S_0$  or  ${}^1D_2$ . The first case is special, since here  $(SL00|JM) = (1100|10) = 0$ . Only in this case eq. (4) yields a  $\sin\Theta_\pi$  dependence for the angular distribution of the pion originating from the  $D_{21}$  decay — exactly what is needed for the description of the data for the  $\pi^+$  angular distribution.

In fact, if we add such a resonance with the processes

$$\begin{aligned} pp \rightarrow D_{21}^{+++}\pi^- \rightarrow \Delta^{++}p\pi^- \rightarrow pp\pi^+\pi^- & \quad (5) \\ pp \rightarrow D_{21}^+\pi^+ \rightarrow \Delta^0p\pi^+ \rightarrow pp\pi^+\pi^- & \end{aligned}$$

with fitted mass  $m_{D_{21}} = 2140$  MeV and width  $\Gamma_{D_{21}} = 110$  MeV, we obtain a good description of the total cross section by adjusting the strength of the assumed resonance process to the total cross section data (solid line in Fig. 4). Simultaneously, the addition of this resonance process provides a quantitative description of all differential distributions (solid lines in Figs. 5 - 9), in particular also of the  $\Theta_{\pi^+}^{c.m.}$ ,  $M_{p\pi^-}$  and  $M_{pp\pi^-}$  distributions. Due to isospin coupling the branch via  $\Delta^0$  is very small and yields only marginal contributions to the observables. Since therefore the  $D_{21}$  decay populates practically only  $\Delta^{++}$ , its reflexion in the  $M_{p\pi^-}$  spectrum shifts the strength to lower masses — as required by the data. The same holds for the  $M_{pp\pi^-}$  spectrum. We are not aware of any other mechanism, which could provide an equally successful description of the observables of the  $pp \rightarrow pp\pi^+\pi^-$  reaction at the energies of interest here.

We note that the only other place in pion production, where a concave curved pion angular distribution has been observed, is the  $pp \rightarrow pp\pi^0$  reaction in the region of single  $\Delta$  excitation [48, 49]. Also in this case it turned out that the reason was the excitation of resonances in the  $\Delta N$  system [49] causing a proton spinflip situation. In general, t-channel resonance excitations are connected with pions emerging in s- or p-waves in non-spinflip configurations and hence lead to flat-to-convex shaped angular distributions.

Also the description of the  $\pi^-$  angular distribution improves by inclusion of the  $D_{21}$  resonance scenario. Whereas the "modified" Valencia calculations predict still a distribution, which is significantly convex, the full calculations, which include the  $D_{21}$  reaction amplitude with  $\pi^-$  particles emerging in relative s-wave, predict a much flatter angular distribution in agreement with the measurements.

At the low-energy side of the beam-energy interval covered by our data the  $D_{21}$  resonance contributes nearly 60% to the total cross section shrinking slightly to less than 50% at the high-energy end. Hence we expect to observe no substantial changes in the differential distributions of  $\Theta_{\pi^+}^{c.m.}$ ,  $M_{p\pi^-}$  and  $M_{pp\pi^-}$ , just a smooth transition from a more to a somewhat less  $D_{21}$  dominated scenario. In Figs. 7 - 9 we plot the three crucial distributions together with their counterparts for the bins at lowest, central and highest energy. Indeed, we observe no significant changes, just a smooth transition of strength

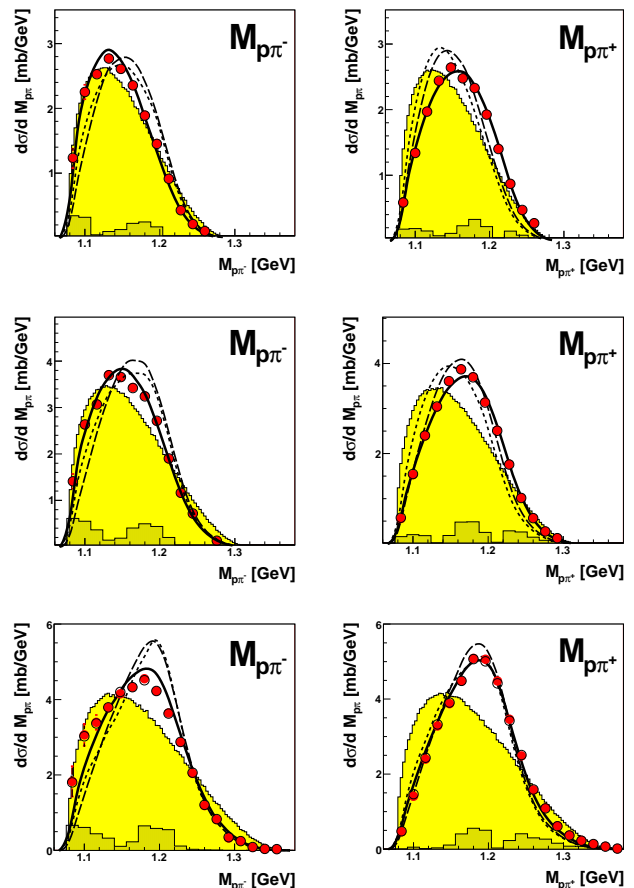


FIG. 7: (Color online) Same as Fig. 5, but for the differential distributions of the invariant-masses  $M_{p\pi^-}$  (left) and  $M_{p\pi^+}$  (right) for the energy bins at  $T_p = 1.10$  (top), 1.18 (middle) and 1.31 GeV (bottom).

to higher masses in the  $M_{p\pi}$  and  $M_{pp\pi}$  spectra. Simultaneously we observe for the  $\Theta_{\pi^+}^{c.m.}$  distribution the transition from a pronounced concave shape at the low-energy bin to a slightly flatter distribution at the high-energy bin. The observed smooth energy dependence of differential distributions is in accord with the  $D_{21}$  hypothesis (solid lines in Figs. 7 - 9). Unfortunately, there are no such data available for the energy region  $T_p = 0.9 - 1.0$  GeV, where due to the opening of the  $D_{21}$  channel the changes in these spectra are expected to be much bigger.

If this scenario is correct, then the  $D_{21}$  contribution of nearly 50% should also persist to higher energies and impress its specific features on the differential observables. Though there are no high-statistics data, there exist at least two bubble-chamber measurements at  $T_p = 1.37$  [2] and 2.0 GeV [6], which show a few differential distributions. Despite limited statistics their  $M_{p\pi^+}$  and  $M_{p\pi^-}$  spectra clearly exhibit the same trend as we observe, namely a strongly excited  $\Delta^{++}$  resonance in combination with a much reduced  $\Delta^0$  excitation.



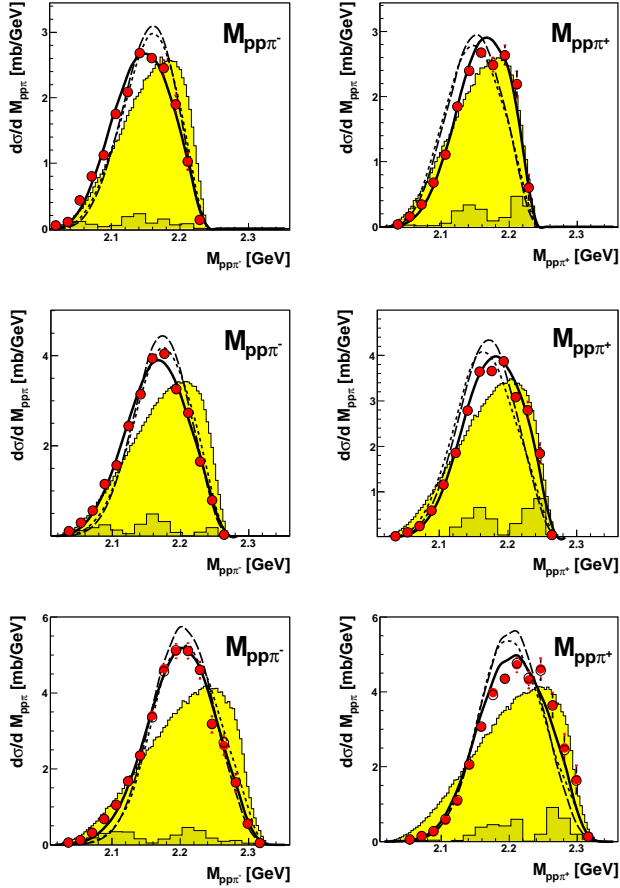


FIG. 8: (Color online) Same as Fig. 5, but for the differential distributions of the invariant-masses  $M_{pp\pi^-}$  (left) and  $M_{pp\pi^+}$  (right) for the energy bins at  $T_p = 1.10$  (top), 1.18 (middle) and 1.31 GeV (bottom).

Though the addition of an isotensor dibaryon resonance cures the shortcomings of the "modified Valencia" calculations for the  $pp \rightarrow pp\pi^+\pi^-$  reaction, we have to investigate, whether such an addition leads to inconsistencies in the description of other two-pion production channels, since such a state may decay also into  $NN\pi$  channels other than  $pp\pi^+$  — though with a much smaller branchings due to isospin coupling. In consequence it may also contribute to other two-pion production channels. This is particularly relevant for the  $pp \rightarrow pp\pi^0\pi^0$  reaction with its comparatively small cross section at the energies of interest here. But the  $D_{21}$  production via the  $^3P_1$  partial wave leaves the two pions in relative  $p$ -wave, hence they are also in an isovector state by Bose symmetry. Since such a  $\rho$ -channel situation is not possible for identical pions, there are no contributions from  $D_{21}$  in  $pp\pi^0\pi^0$  and  $nn\pi^+\pi^+$  channels, *i.e.* there is no consistency problem.

From a fit to the data we obtain a mass  $m_{D_{21}} = 2140(10)$  MeV and a width  $\Gamma_{D_{21}} = 110(10)$  MeV. The

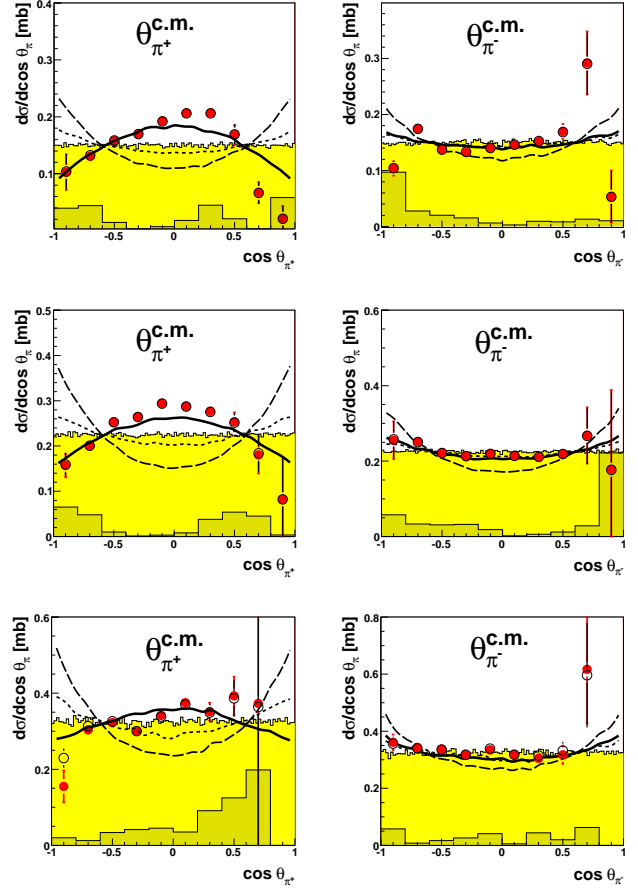


FIG. 9: (Color online) Same as Fig. 5, but for the differential distributions of the pion angles  $\theta_{\pi^+}^{c.m.}$  (left) and  $\theta_{\pi^-}^{c.m.}$  (right) for the energy bins at  $T_p = 1.10$  (top), 1.18 (middle) and 1.31 GeV (bottom).

mass is in good agreement with the prediction of Dyson and Xuong [35]. From their Faddeev calculations Gal and Garcilazo [37] obtain slightly larger values for mass and width. The extracted mass and width of the  $D_{21}$  state coincide with those for the  $D_{12}$  state. This means that the masses of this dibaryon multiplet do not exhibit any particular isospin dependence — just as assumed in the work of Dyson and Xuong.

Possibly this resonance was sensed already before in the pionic double charge exchange reaction on nuclei. There the so-called non-analog transitions exhibit an unexpected resonance-like behavior in the region of the  $\Delta$  resonance [36, 47, 50]. For its explanation the DINT mechanism [52–55] was introduced, which in essence can be imagined as representing a  $\Delta N$  system with  $I(J^P) = 2(1^+)$  in the intermediate state [54].

## V. SUMMARY AND CONCLUSIONS

Total and differential cross sections of the  $pp \rightarrow pp\pi^+\pi^-$  reaction have been measured exclusively and kinematically complete in the energy range  $T_p = 1.08 - 1.36$  GeV ( $\sqrt{s} = 2.35 - 2.46$  GeV) by use of the quasi-free process  $pd \rightarrow pp\pi^+\pi^- + n_{spectator}$ . The results for the total cross section are in good agreement with previous bubble-chamber data. For the differential cross sections no data from previous measurements are available.

The original Valencia calculations describing Roper and  $\Delta\Delta$  excitations by  $t$ -channel meson exchange account well for the total cross section, but fail badly for the differential distributions of the  $pp \rightarrow pp\pi^+\pi^-$  reaction. These calculations also have been shown to fail in other two-pion production channels, both for total and differential cross sections.

The differential cross sections for the  $pp \rightarrow pp\pi^+\pi^-$  reaction are somewhat better accounted for by the "modified Valencia" calculations, but still fail strikingly for the  $M_{p\pi^-}$ ,  $M_{pp\pi^-}$  and  $\Theta_{\pi^+}^{c.m.}$  distributions. These calculations, which were tuned to the  $pp \rightarrow pp\pi^0\pi^0$  and  $pp \rightarrow nn\pi^+\pi^+$  reactions, have been shown to do well in the description of the other two-pion channels both in total and in differential cross sections. However, these so far very successful calculations predict also a much too small total cross section for the  $pp\pi^+\pi^-$  channel at energies above  $T_p \approx 0.9$  GeV.

This failure can be cured, if there is an opening of

a new reaction channel near  $T_p \approx 0.9$  GeV, *i.e.*, near the  $\Delta N\pi$  threshold, which nearly exclusively feeds the  $pp\pi^+\pi^-$  channel. Such a process is the associated production of the isotensor  $\Delta N$  state  $D_{21}$  with specific signatures in invariant mass spectra and in the  $\pi^+$  angular distribution. We have demonstrated that such a process provides a quantitative description of the data for the  $pp \rightarrow pp\pi^+\pi^-$  reaction — both for the total cross section and for all differential distributions.

This  $D_{21}$  state has been predicted already in 1964 by Dyson and Xuong [35] and more recently by Gal and Garcilazo [37], who also calculated its decay width. It is remarkable that five out of the six dibaryon states predicted in 1964 by considering  $SU(6)$  symmetry breaking have now been verified with masses very close to the predicted ones. For the sixth state,  $D_{30}$ , only upper limits have been found so far [56], but this subject deserves certainly further, more detailed investigations.

## VI. ACKNOWLEDGMENTS

We acknowledge valuable discussions with A. Gal, Ch. Hanhart, V. Kukulín and G. J. Wagner on this issue. We are particularly indebted to L. Alvarez-Ruso for using his code. This work has been supported by DFG (CL214/3-1 and 3-2) and STFC (ST/L00478X/1) as well as by the Polish National Science Centre through the grant 2016/23/B/ST2/00784.

- 
- [1] L. G. Dakhno *et al.*, Sov. J. Nucl. Phys. **37** (1983) 540
  - [2] C. D. Brunt, M. J. Clayton and B. A. Wetswood, Phys. Rev. **187** (1969) 1856
  - [3] F. Shimizu *et al.*, Nucl. Phys. A **386** (1982) 571
  - [4] V. V. Sarantsev *et al.*, Phys. At. Nucl. **70** (2007) 1885
  - [5] A. M. Eisner *et al.*, Phys. Rev. **138** (1965) B670
  - [6] E. Pickup, D. K. Robinson and E. O. Salant, Phys. Rev. **125** (1962) 2091
  - [7] T. Tsuboyama, F. Sai, N. Katayama, T. Kishida and S. Yamamoto, Phys. Rev. C **62** (2000) 0340011
  - [8] W. Brodowski *et al.*, Phys. Rev. Lett. **88** (2002) 192301
  - [9] J. Johanson *et al.*, Nucl. Phys. A **712** (2002) 75
  - [10] J. Pätzold *et al.*, Phys. Rev. C **67** (2003) 052202
  - [11] T. Skorodko *et al.*, Eur. Phys. J. A **35** (2008) 317
  - [12] T. Skorodko *et al.*, Phys. Lett. B **679** (2009) 30
  - [13] F. Kren *et al.*, Phys. Lett. B **684** (2010) 110 and Phys. Lett. B **702** (2011) 312; arXiv:0910.0995[nucl-ex]
  - [14] T. Skorodko *et al.*, Phys. Lett. B **695** (2011) 115
  - [15] T. Skorodko *et al.*, Eur. Phys. J. A **47** (2011) 108
  - [16] M. Bashkanov *et al.*, Phys. Rev. Lett. **102** (2009) 052301.
  - [17] P. Adlarson *et al.*, Phys. Lett. B **706** (2012) 256
  - [18] S. Abd El-Samad *et al.*, Eur. Phys. J. A **42** (2009) 159
  - [19] S. Abd El-Bary *et al.*, Eur. Phys. J. A **37** (2008) 267
  - [20] P. Adlarson *et al.* Phys. Rev. Lett. **106** (2011) 242302.
  - [21] P. Adlarson *et al.*, Eur. Phys. J. A **52** (2016) 147
  - [22] P. Adlarson *et al.*, Phys. Lett. B **721** (2013) 229
  - [23] P. Adlarson *et al.*, Phys. Rev. C **88** (2013) 055208
  - [24] P. Adlarson *et al.*, Phys. Lett. B **743** (2015) 325
  - [25] G. Agakishiev *et al.*, Phys. Lett. B **750** (2015) 184
  - [26] A. P. Jerusalimov *et al.*, Eur. Phys. J. A **51** (2015) 83
  - [27] H. Clement, M. Bashkanov and T. Skorodko, Phys. Scr. T **166** (2015) 014016
  - [28] P. Adlarson *et al.*, Phys. Rev. Lett. **112** (2014) 202301.
  - [29] P. Adlarson *et al.*, Phys. Rev. C **90** (2014) 035204.
  - [30] R. L. Workman, W. J. Briscoe and I. I. Strakovsky, Phys. Rev. C **93** (2016) 045201
  - [31] L. Alvarez-Ruso, E. Oset, E. Hernandez, Nucl. Phys. A **633** (1998) 519 and priv. comm.
  - [32] X. Cao, B.-S. Zou and H.-S. Xu, Phys. Rev. C **81** (2010) 065201
  - [33] A. V. Anisovich *et al.*, Eur. Phys. J. A **48** (2012) 15
  - [34] K. A. Olive *et al.* (PDG), Chin. Phys. C **38** (2014) 090001.
  - [35] F. J. Dyson and N.-H. Xuong, Phys. Rev. Lett. **13** (1964) 815.
  - [36] H. Clement, Prog. Part. Nucl. Phys. **93** (2017) 195
  - [37] A. Gal and H. Garcilazo, Nucl. Phys. A **928** (2014) 73
  - [38] P. Adlarson *et al.*, arXiv:1803.03193 [nucl-ex]
  - [39] Ch. Bargholtz *et al.*, Nucl. Instrum. Methods A **547** (2005) 294.
  - [40] H. H. Adam *et al.*, arXiv:nucl-ex/0411038 (2004).
  - [41] R. Machleidt, Phys. Rev. C **63** (2001) 024001.
  - [42] P. Adlarson *et al.*, Phys. Rev. C **91** (2015) 015201
  - [43] M. Bashkanov and H. Clement, Eur. Phys. J. A **50** (2014) 107

- [44] N. Hoshizaki, *Prog. Theor. Phys.* **89** (1993) 251
- [45] R. A. Arndt, J. S. Hyslop and L. D. Roper, *Phys. Rev. D* **35** (1987) 128
- [46] M. Bashkanov, H. Clement and T. Skorodko, *Nucl. Phys. A* **958** (2017) 129
- [47] H. Clement, *Prog. Part. Nucl. Phys.* **29** (1992) 175
- [48] S. Abd El-Samad *et. al.*, *Eur. Phys. J. A* **30** (2006) 443
- [49] V. Komarov *et. al.*, *Phys. Rev. C* **93** (2016) 065206
- [50] M. B. Johnson and C. L. Morris, *Ann. Rev. Part. Sci.* **43** (1993) 165
- [51] R. Gilman *et al.*, *Phys. Rev. C* **35** (1987) 1334
- [52] Mikkel B. Johnson, E. R. Siciliano, H. Toki and A. Wirzba, *Phys. Rev. Lett.* **52** (1984) 593
- [53] R. Gilman, H. T. Fortune, M. B. Johnson, E. R. Siciliano, H. Toki and A. Wirzba, *Phys. Rev. C* **32** (1985) 349
- [54] Mikkel B. Johnson and L. S. Kisslinger, *Phys. Lett. B* **168** (1986) 26
- [55] A. Wirzba, H. Toki, E. R. Siciliano, M. B. Johnson and R. Gilman, *Phys. Rev. C* **40** (1989) 2745
- [56] P. Adlarson *et. al.*, *Phys. Lett. B* **762** (2016) 455
- [57] neglecting a very small contribution from the Roper decay branch  $N^* \rightarrow \Delta\pi$